HOSTED BY

ELSEVIER

CrossMark

Available online at www.sciencedirect.com

ScienceDirect

Radiology of Infectious Diseases 3 (2016) 66–73

www.elsevier.com/locate/jrid

Research article

Imaging findings of *Paragonimus westermani*

Shambhu Kumar Sah [a], Silin Du [a], Yi Liu [a], Ping Yin [a], Oormila Ganganah [b], Manu Chiniah [c], Pranesh Kumar Yadav [d], You You Guo [a], Yongmei Li [a,*]

[a] *Department of Radiology, The First Affiliated Hospital of Chongqing Medical University, No. 1 Youyi Road, Yuzhong District, Chongqing 400016, China*
[b] *Department of Respiratory Medicine, The First Affiliated Hospital of Chongqing Medical University, No. 1 Youyi Road, Yuzhong District, Chongqing 400016, China*
[c] *Department of General Surgery, The First Affiliated Hospital of Chongqing Medical University, No. 1 Youyi Road, Yuzhong District, Chongqing 400016, China*
[d] *Department of Orthopedics, The Second Affiliated Hospital of Chongqing Medical University, Yuzhong District, Chongqing 400016, China*

Received 21 January 2016; revised 22 January 2016; accepted 22 January 2016
Available online 4 March 2016

Abstract

Purpose: To analyze the imaging findings of pulmonary and extra-pulmonary paragonimiasis.
Methods: The imaging findings of serologically and clinically confirmed 22 cases of *Paragonimus westermani* infection identified over a five-year period (2010–2015) were retrospectively analyzed. Chest CT (n = 22), brain CT (n = 2) & MRI (n = 1), abdomen CT (n = 3) scans were available.
Results: Chest CT scan was abnormal in 20 patients and the CT findings were as follows: nodule (n = 18), ground glass opacity (GGO) (n = 12), worm cyst (n = 10), migration track (n = 7), fibrosis (n = 5), pleural effusion (n = 15), pleural thickening (n = 10), pleural calcification (n = 1). Hilar or mediastinal lymphadenopathy was noted in three patients. Brain CT scan showed patchy low density in the left occipital lobe in one patient and patchy mixed density in the right basal ganglia and kidney-shaped low density area in the left basal ganglia in another patient. Brain MRI scan revealed a circular lesion with ring enhancement in the right parietal lobe. Abdominal CT scan showed conglomerated small cystic or serpentine lesions and migration track in the right lobe of liver and spleen.
Conclusions: The imaging findings of *P. westermani* is so diverse and non-specific due to its complex life cycle and several life stages during infestation of human; however, common features include nodule, GGO, worm cyst, migration track, pleural effusion, pleural thickening on chest CT scan; patchy low or mixed density lesions on brain CT scan; ring enhancing lesion on brain MRI scan; conglomerated small cystic or serpentine lesions and migration track in liver and spleen on abdominal CT scan. The characteristic imaging features of paragonimiasis are worm cyst and migration track.

Keywords: Paragonimiasis; Imaging findings; Chest; Brain; Abdomen

1. Introduction

Paragonimiasis, the oriental lung fluke disease, is an important food-borne parasitic zoonosis caused by various species of the trematode genus *Paragonimus*. It is endemic in many parts of Asia, Africa, and South America [1]. In recent years, it has emerged worldwide due to increase in the number of travelers and the expansion of food trading. The estimated number of people infected with the human lung fluke is 23 million globally [2], with 293 million people at risk for

* Corresponding author. Tel.: +86 23 68899931, +86 13101363092 (cell); fax: +86 23 68811487.
E-mail addresses: mrsks2007@hotmail.com (S.K. Sah), 182389558@qq.com (S. Du), liuyi653044@163.com (Y. Liu), yinping915@163.com (P. Yin), oormilaganganah@yahoo.com (O. Ganganah), manu_chiniah@hotmail.com (M. Chiniah), dr.pranesh11@yahoo.com (P.K. Yadav), 1272378153@qq.com (Y.Y. Guo), lymzhang70@aliyun.com (Y. Li).
Peer review under responsibility of Beijing You'an Hospital affiliated to Capital Medical University.

http://dx.doi.org/10.1016/j.jrid.2016.01.008

infection with *Paragonimus* species [3]. In the genus *Paragonimus*, there are more than 50 different species of which 9 are known to cause infections in humans [4]. *Paragonimus westermani* is the best known species which is widely distributed human pathogen in Asia.

Freshwater snails and crustaceans (crabs or crayfish) are the first and second intermediate hosts, respectively. Human infection results from ingestion of uncooked or inadequately cooked crustaceans containing metacercariae, the infective stage of the parasite. Although primary site of paragonimiasis is the lung, extra-pulmonary infections can occur in brain, spinal cord, liver, spleen, ovary, etc [5–7]. Pulmonary paragonimiasis is usually misdiagnosed as pneumonia, tuberculosis, or lung cancer. Extra-pulmonary paragonimiasis is a relatively rare form of paragonimiasis.

To our knowledge, no imaging findings of patients showing chest, brain and abdominal features at the same time have been reported, except for a few case reports describing the disseminated form of paragonimiasis. Recognition and understanding the spectrum of imaging findings of *P. westermani* infection can aid in the diagnosis. In this study, we retrospectively reviewed the imaging findings of 22 cases of *P. westermani* infection in an effort to further characterize the disease for early diagnosis and institution of appropriate treatment to achieve a favorable prognosis.

2. Materials and methods

2.1. Patients

We retrospectively analyzed the imaging findings of serologically and clinically confirmed 22 cases of *P. westermani* infection identified over a five-year period (2010–2015) in two institutions. The institutional review board of hospitals approved the study and did not require additional informed patient consent for reviewing the patient's medical records and images. We also reviewed English-language literature on paragonimiasis based on PubMed records.

2.2. Radiological examination

All the 22 patients received chest CT scanning. Two patients underwent brain CT scanning and another 1 patient received MR imaging of the brain with contrast enhancement. Abdominal CT scanning with contrast enhancement was done in three patients. The images were retrospectively evaluated by consensus of two experienced radiologists who were unaware of the final diagnosis of the patients on a local picture archiving and communication system (PACS) monitor.

Pulmonary nodule was defined as a round or ovoid soft-tissue opacity measuring <3 cm in diameter. Ground glass opacity (GGO) was defined as hazy increased attenuation of the lung with preserved bronchovascular markings. Worm cyst was defined as round cystic areas consisting fluid or gas. Migration track was defined as tubular and linear structures that showed a tortuous course. Lymphadenopathy was considered positive when the shortest diameter of a lymph node was greater than 1 cm.

2.3. Laboratory tests

Laboratory tests of blood included complete blood counts (CBC), erythrocyte sedimentation rate (ESR), c-reactive protein (CRP), routine biochemistry analysis. Mantoux test or purified protein derivative (PPD) skin test was done in six patients. Sputum examinations were performed in eight patients and stool examinations were performed in five patients. Serological test was done in all patients.

3. Results

3.1. Clinical features

Our study included 22 patients (18 males and 4 females; age range 9–49 years; mean age 26.27 years) with serologically and clinically confirmed paragonimiasis. Clinical presentations were dry cough (n = 9), productive cough (n = 8), fever (n = 6), chest pain (n = 6), dyspnea (n = 4), headache (n = 3), vomiting (n = 2), abdominal pain (n = 2), diarrhea (n = 1). Wheezing was observed in five patients. Eight patients had a history of eating freshwater crabs.

3.2. Imaging findings

The imaging findings of *P. westermani* for all patients are summarized in Table 1. Chest CT scan was abnormal in 20 patients and the CT findings were as follows: nodule (n = 18) (Figs. 1A and 4A), ground glass opacity (GGO) (n = 12) (Fig. 2B), worm cyst (n = 10) (Figs. 2A, 4B and 5A), migration track (n = 7) (Fig. 1B), fibrosis (n = 5), pleural effusion (n = 15), pleural thickening (n = 10), pleural calcification (n = 1). Hilar or mediastinal lymphadenopathy was noted in three patients. The chest CT findings of nodular attenuation with a surrounding halo of hemorrhage seen as an area of ground-glass opacity (halo sign) were observed in three patients (Fig. 2B).

Brain CT scan showed patchy low density in the left occipital lobe in one patient (Fig. 3A) and patchy mixed density in the right basal ganglia and kidney-shaped low density area in the left basal ganglia in another patient (Fig. 3B). Brain MRI scan revealed a circular area (diameter 6 mm) of mixed signals with ring-shaped low T2 signal in the right parietal lobe (Fig. 4C). Flow void, hemorrhage and surrounding edema were also seen. Ring enhancement was seen after contrast administration (Fig. 4D). Abdominal CT scan showed conglomerated small cystic or serpentine lesions and migration track in the right lobe of liver (Fig. 5B) and spleen (Fig. 5C, D). One patient had simultaneous involvement of lung, pleura, liver and spleen. The characteristic imaging features of paragonimiasis are worm cyst and migration track.

In our study, 7 cases have been misdiagnosed as either tuberculosis, or tumor, or fungal infection radiologically and

Table 1
Imaging findings of *Paragonimus westermani*.

Case	Sex/age (year)	Radiological modality	Imaging findings
1	M/21	Chest CT	Nodule, worm cyst, ground glass opacity (GGO), pleural effusion, pleural thickening, pleural calcification
		Abdomen CT	Conglomerated small cystic or serpentine lesions and migration track in the right lobe of liver and spleen.
2	M/9	Chest CT	Nodule, worm cyst, GGO, pleural effusion, lymphadenopathy
		Brain MRI	A circular lesion with ring enhancement in the right parietal lobe.
3	M/15	Brain CT	Patchy low density in the left occipital lobe.
4	M/16	Chest CT	Nodule, worm cyst, migration track, GGO, pleural effusion, pleural thickening
5	M/39	Chest CT	Nodule, worm cyst, GGO, pleural thickening
6	M/29	Chest CT	Nodule, pleural effusion, fissural thickening, fibrosis
7	M/21	Chest CT	Migration track, pleural effusion, pleural thickening and adhesion, GGO, fibrosis
8	F/15	Chest CT	Nodules, pleural effusion
		Abdomen CT	Liver: Conglomerated small cystic and serpentine lesions
9	M/45	Chest CT	Nodule, pleural effusion, fissural thickening
10	M/47	Chest CT	Nodule, migration track, pleural thickening and adhesion, fibrosis, lymphadenopathy
11	M/38	Brain CT	Patchy mixed density in the right basal ganglia and kidney-shaped low density area in the left basal ganglia.
12	M/39	Chest CT	Nodule, worm cyst, GGO, pleural effusion, pleural thickening, fissural thickening
13	F/49	Chest CT	Nodule, pleural effusion, pleural thickening
14	M/14	Chest CT	Nodule, worm cyst, GGO, pleural effusion, lymphadenopathy
		Abdomen CT	Liver: Conglomerated small cystic or serpentine lesions and migration track in the right lobe of liver
15	M/22	Chest CT	Nodules, pleural effusion
16	M/18	Chest CT	Nodule, worm cyst, GGO, pleural thickening
17	M/34	Chest CT	Migration track, pleural thickening, fibrosis
18	F/26	Chest CT	Nodule, GGO, pleural effusion
19	M/42	Chest CT	Nodule, worm cyst, GGO, pleural thickening, fibrosis
20	M/12	Chest CT	Nodule, worm cyst, GGO, migration track, pleural effusion
21	F/14	Chest CT	Nodules, migration track, pleural effusion
22	M/13	Chest CT	Nodule, worm cyst, GGO, migration track, pleural effusion

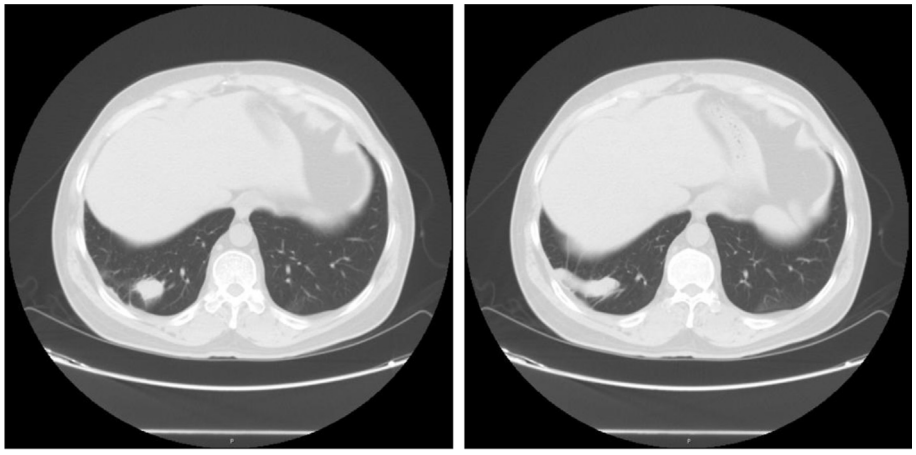

Fig. 1. A 47-year-old man with pulmonary paragonimiasis in right lower lobe. Plain CT scan of chest shows a pulmonary nodule (A), and a tubular opacity extending from the pleura to the lung, which suggests a migration track (B).

the diagnosis was delayed. Three patients even received anti-tuberculosis therapy based on radiological diagnosis.

3.3. Laboratory findings

CBC showed increased white blood count (WBC) with relative lymphocytosis in nine patients. Eosinophilia (absolute eosinophil count > 1000/μl) was found in all patients. Elevated ESR was seen in 10 patients; however CRP was normal in all patients. Three patients showed positive PPD skin tests. However, three sputum acid-fast bacillus (AFB) smears showed negative results for pulmonary tuberculosis. *Paragonimus* eggs were not seen in stool examinations. Enzyme-linked immunosorbent assay (ELISA) was positive for antibodies against *P. westermani* in all patients.

All patients were treated with antihelminthic drug (praziquantel) and remained well after a complete course of treatment.

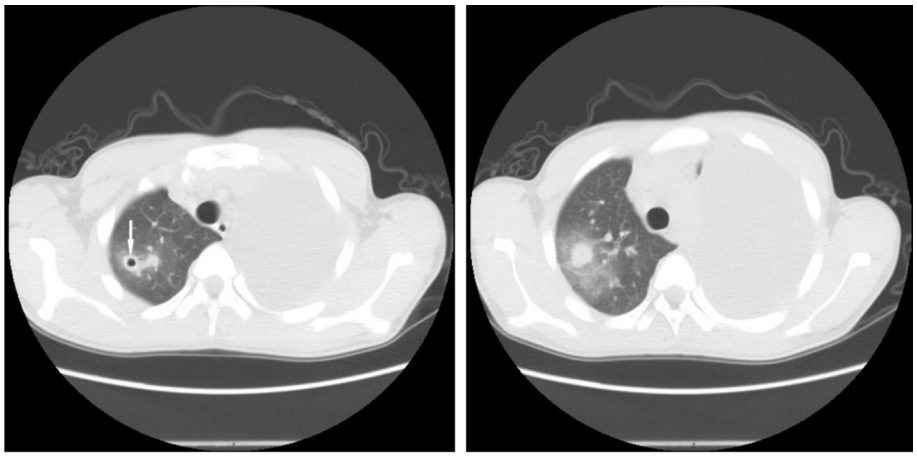

A B

Fig. 2. A 16-year-old boy with pulmonary paragonimiasis. Plain CT scan of chest shows worm cyst within the nodule (arrow) (A), and ground glass opacity surrounding the nodule (halo sign) in right upper lobe (B). Atelectasis of left lung due to massive pleural effusion can be seen.

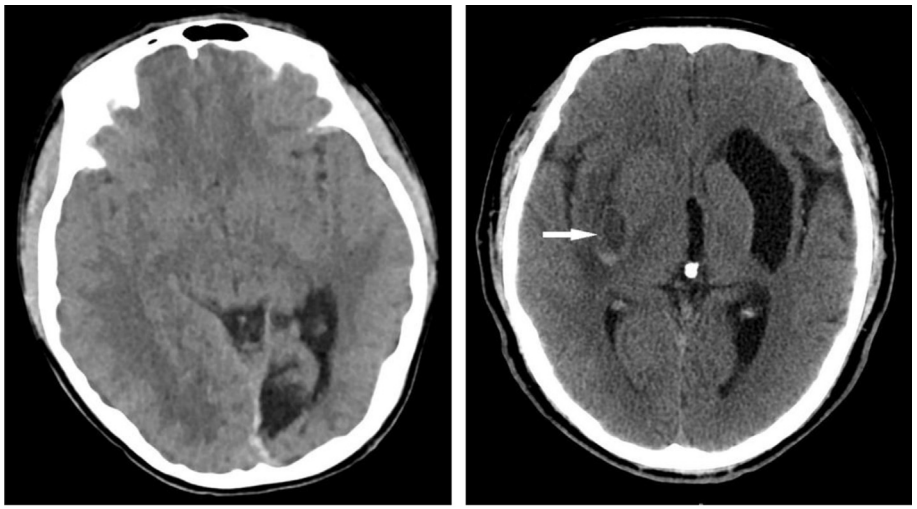

A B

Fig. 3. (A) A 15-year-old boy with cerebral paragonimiasis. Plain CT scan of brain shows patchy low density in the left occipital lobe. (B) A 38-year-old man with cerebral paragonimiasis. Plain CT scan of brain shows patchy mixed density in the right basal ganglia (arrow) and kidney-shaped low density area in the left basal ganglia.

4. Discussion

Human paragonimiasis is an important parasitic lung fluke infection caused by the genus *Paragonimus*. *P. westermani* is the most common and widely distributed species in Asian countries. It has a complex life cycle including intermediate developmental stages in snails and crustaceans [1]. Human acquire infection by ingestion of uncooked or inadequately cooked crustaceans containing metacercariae, the infective stage of the parasite [8]. The metacercariae excyst in the small intestine, migrate through the intestinal wall and enter the abdominal cavity. Next they penetrate the diaphragm and pleura and enter the lung in three to eight weeks, where they develop into the adult worms. In our study, only eight patients had a history of eating freshwater crabs. However, contamination of fingers with metacercariae might occur while cooking the crabs, and the chopping board or other cooking utensils might also be contaminated. Wild boar meat is a principal source of human infection in Western Japan, particularly, the two Southern prefectures of Kyushu Island, where 30.5% of paragonimiasis in Japan in 2001–2012 occurred [9].

Clinically, paragonimiasis may be categorized into pulmonary, pleuropulmonary and extra-pulmonary forms. Alternatively, it can also be classified into acute and chronic paragonimiasis and ectopic paragonimiasis [1]. Extra-pulmonary paragonimiasis, an uncommon lung fluke disease, is usually reported to occur following pulmonary paragonimiasis. In our study, sixteen patients had only pulmonary paragonimiasis; four patients suffered from both pulmonary

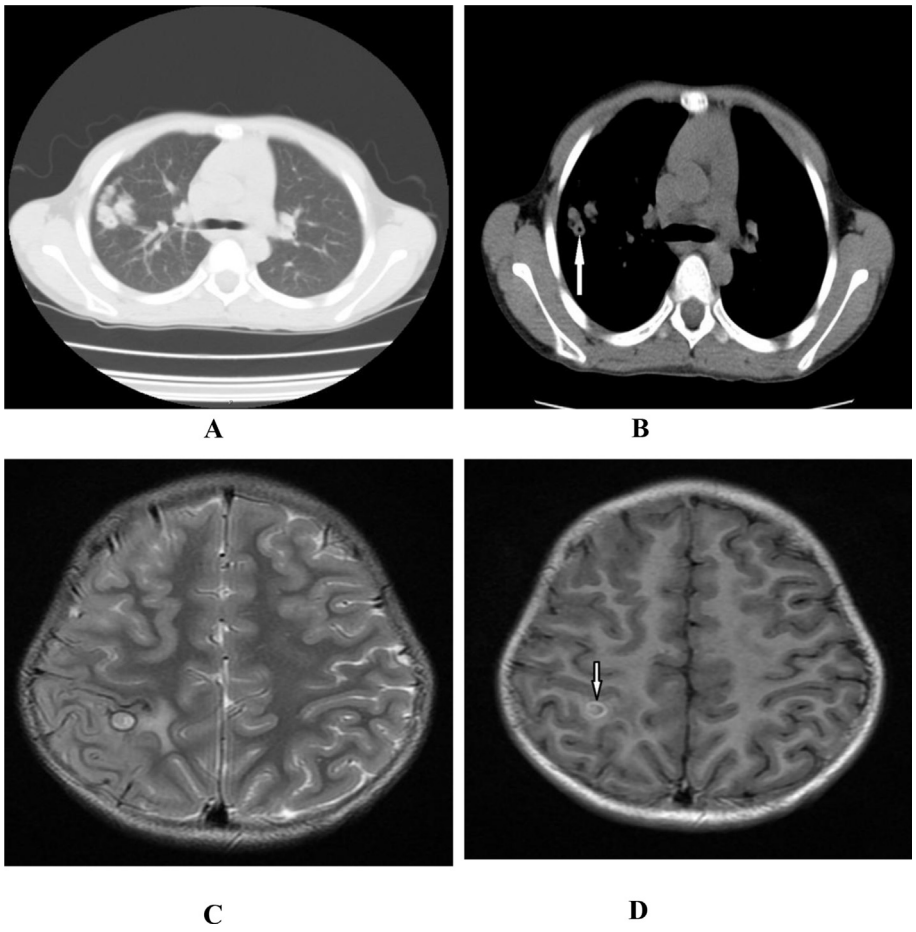

Fig. 4. A 9-year-old boy with both pulmonary and cerebral paragonimiasis. Plain CT scan of chest shows a complex of multiple nodules (A) and worm cyst within the nodule (arrow) (B). Brain MRI shows a circular area (diameter 6 mm) of mixed signals with ring-shaped low T2 signal in the right parietal lobe; flow void, hemorrhage and surrounding edema can also be seen (C). Ring enhancement was seen after contrast administration (arrow) (D).

and extra-pulmonary paragonimiasis; two patients with only cerebral paragonimiasis.

It frequently affects men than women and is common in children [10]. In our study, 18 patients out of 22 were male indicating male predominance and eight patients were below 16 years old. Generally the parasites undergo several life stages during infestation of humans. Therefore, the involved sites, clinical presentations, and imaging findings may depend on these stages. The incubation period may vary from 1 to 2 months or even longer. Pulmonary paragonimiasis is usually associated with infections in the pleura, diaphragm, and thoracic cavity. It is mainly manifested with dry cough initially then productive cough, fever, chest pain, and dyspnea. Pulmonary paragonimiasis presenting with hemoptysis was generally mistaken for sputum smear negative pulmonary tuberculosis or some other serious conditions [11]. No patients in our series presented with hemoptysis. Cerebral paragonimiasis is the most common and serious form of extra-pulmonary paragonimiasis. The common clinical manifestations include seizure (especially Jacksonian type), headache, vomiting, visual disturbance, and motor weakness [12]. However, our patients with cerebral paragonimiasis only presented with headache and vomiting. Abdominal paragonimiasis is a relatively rare form, mainly manifested as abdominal pain, nausea, vomiting, and diarrhea.

Chest radiography revealed patchy consolidations in 62–71%, nodules in 8–13%, cystic or cavitary lesions in 11–14%, pleural effusion in 9–10%, and pleural thickening in 28% [13]. Higher rate of normal chest radiographs were reported in pulmonary paragonimiasis [14]. CT is the imaging modality of choice for paragonimiasis because it permits visualization of the frequently involved sites (i.e. lung and pleura) including brain and solid abdominal organs, gastrointestinal tract and peritoneal cavity. In a study by Im et al. [15], the characteristic CT features of pulmonary paragonimiasis were round low attenuation cystic lesions filled with fluid or gas. CT scan showed air-space consolidation in 82%, nodules in 41%, worm migration track in 41%, and bronchiectasis in 35%. The prevalence of pleural effusion in pulmonary paragonimiasis varies from 2.9% to 54% [16,17]. Paragonimiasis has been re-emerging in Japan since the 1980s [18] due to the increased number of infected immigrants with predominant finding of pleurisy (58.2%) such as pneumothorax or pleural effusion [19]. Pleurisy with relatively high eosinophilia and dominant immunoglobulin (Ig) M antibody are characteristic features of the early stage of paragonimiasis, whereas

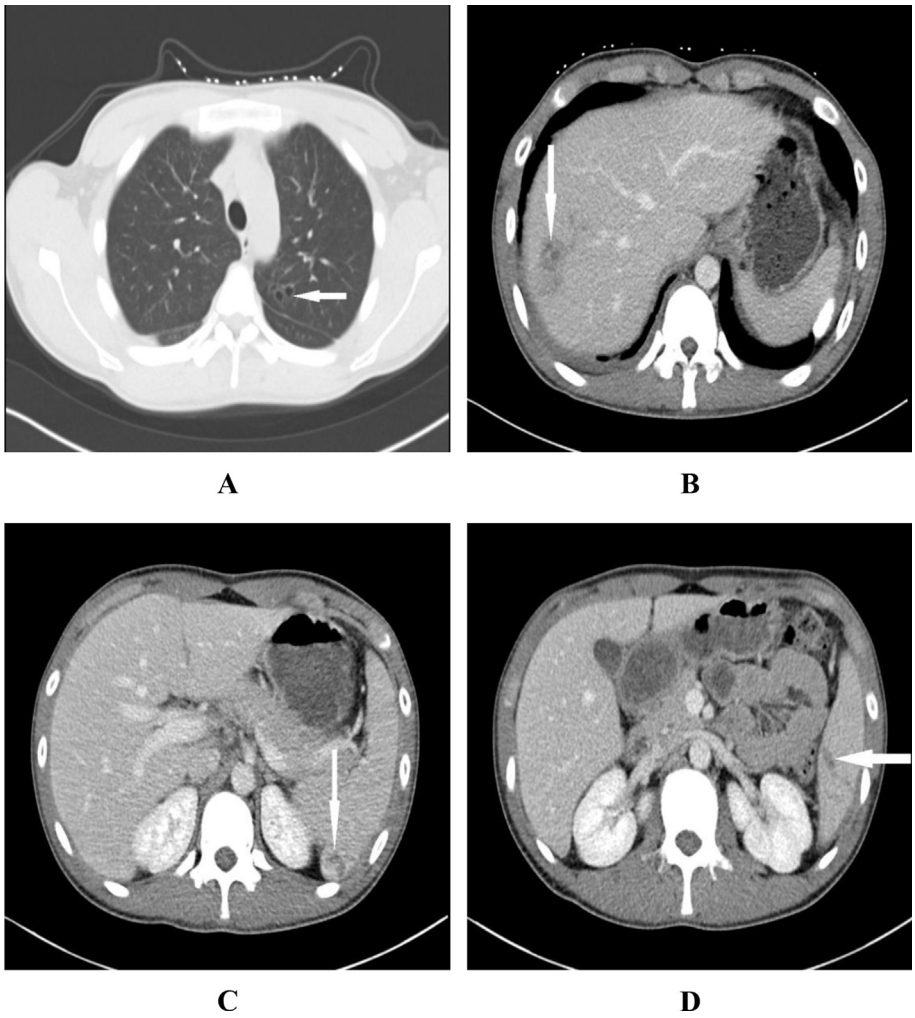

Fig. 5. A 21-year-old man with both pulmonary and abdominal paragonimiasis. Plain CT scan of chest shows multiple thin-walled cystic lesions consisting fluid or gas (worm cysts) (arrow) (A). Contrast-enhanced CT scan of abdomen at portal venous phase shows conglomerated small cystic or serpentine lesions and tubular low-attenuated lesions (migration track) in the right lobe of liver (arrow) (B) and spleen (arrows) (C, D).

parenchymatous lesions in the lungs, with relatively low eosinophilia and dominant IgG antibody, are characteristic of the late stage [20]. The common CT findings of pulmonary paragonimiasis in our series were nodule, ground glass opacity (GGO), worm cyst, migration track, pleural effusion, and pleural thickening. CT and MRI scans of brain of early and late cerebral paragonimiasis depicted as multiple, densely calcified area with round or nodular shapes, surrounded by a large area of low density; cortical atrophy and ventricular dilatation [17]. Chen et al. [21] described the characteristic imaging manifestations of cerebral paragonimiasis as single or clustered ring-like lesions with incommensurate edema surrounding the lesions on enhanced MRI examination. Recently, imaging manifestations of an adult cerebral paragonimiasis with the initial symptom of hemorrhagic stroke depicted as massive edema zone with “ring-like shape” around the hematoma and “tunnel-like shape” in the hematoma [22]. Cerebral paragonimiasis in our study showed patchy low density or mixed density lesions on brain CT scan and a circular lesion with ring enhancement, flow void, hemorrhage and surrounding edema on MRI scan. There were no calcified lesions in our patients indicating early stages of infection. Compare to CT, MRI is a better technique for visualization of the lesions in the brain. Imaging findings of hepatic paragonimiasis can vary from a cluster of small cysts with rim enhancement in the subcapsular area of the liver [23], to peripheral mutually connected cysts with tortuous tract formation, and tubular enhancement [24]. It is also depicted as cystic, linear and serpentine hypodensities in the subcapsular and central areas of the liver [25]. Paragonimiasis may also cause active hepatic capsulitis [26]. Li et al. [6] reported splenic paragonimiasis as multiple irregular low-attenuated patchy areas with fusion tendency, which was surrounded by multiple hypo-attenuated tortuous structures (worm migration track). Conglomerated small cystic or serpentine lesions and migration track in the right lobe of liver and spleen were revealed on abdominal CT scans of our patients with abdominal paragonimiasis. The characteristic imaging features of paragonimiasis are worm cyst and migration track. Singcharoen et al. [27] reported CT findings of disseminated

paragonimiasis, in which multiple cystic lesions were scattered throughout the entire body, including the pleural space, lung parenchyma, mediastinum, liver, abdominal wall, and peritoneal cavity.

Radiologically, sometimes it is difficult to distinguish pulmonary paragonimiasis from pulmonary tuberculosis or tumor or fungal infections due to overlapping imaging features. Nodules, pleural effusion on chest CT scan are also suggestive of pulmonary tuberculosis. Kim et al. [28] reported a case of pulmonary paragonimiasis mimicking metastatic pulmonary tumor by showing a high FDG (fluorodeoxyglucose) uptake on FDG PET (positron emission tomography). CT revealed pleural lesions (62%) and parenchymal lesions (92%) with predominant subpleural solitary nodular lesions, mimicking lung cancer, tuberculosis, or fungal diseases [29]. Recently, Seon et al. [30] reported the presence of internal low attenuation and perilesional centrilobular nodules associated with pulmonary consolidative lesions, along with cavitary lesions and worm-migration tracts, is more frequent in patients with paragonimiasis than in patients with non-paragonimiatic parasite infestation. Singh et al. [31] reported a case of cerebral paragonimiasis mimicking tuberculoma as an isodense area with surrounding edema on the left parietal lobe on brain CT scan. The chest CT 'halo sign' is defined as an area of ground-glass opacity (GGO) surrounding a pulmonary nodule. It was initially described as a sign of hemorrhage around foci of invasive pulmonary aspergillosis [32]. The halo sign is non-specific as it may also accompany with candidiasis, coccidioidomycosis, eosinophilic pneumonia, organizing pneumonia, bronchiolitis obliterans, herpes simplex and cytomegalovirus infection, Wegener granulomatosis, Kaposi sarcoma, bronchoalveolar carcinoma, lymphoma and metastatic angiosarcoma. In our study, CT halo sign was observed in three patients that may represent inflammation or hemorrhage surrounding the worm cyst.

Although CT scan has been advocated as a key consideration in the early diagnosis of paragonimiasis, none of the signs is sensitive or pathognomic. Magnetic resonance imaging (MRI), positron emission tomography (PET) and Ultrasonography (USG) have all been used to evaluate *P. westermani*, but the features are non-specific for paragonimiasis.

Leucocytosis, eosinophilia and elevated ESR were common findings in patients with paragonimiasis [13]. Our study also showed similar laboratory findings and blood eosinophilia as seen in all of our patients is suggestive of parasitic infection at the early stage when the parasites are migrating, but it disappears at the chronic stage of infection. Eosinophilia noted in the serum could be relevant to IL-5 in paragonimiasis. IL-5, a potent eosinophil chemotactic and growth factor, plays a key role in parasite induced eosinophilia. Mantoux test or purified protein derivative (PPD) skin test is a screening test and has a false positive or negative result for tuberculosis. The diagnostic criteria of paragonimiasis are based on clinical history, radiological findings, absolute eosinophilia, positive findings on a serological test, or detection of eggs or worms in sputum or bronchoalveolar lavage (BAL) fluid or stool or in a pathologic specimen [33]. In our study, all patients were confirmed to have *P. westermani* by immunoserological examination using enzyme-linked immunosorbent assay (ELISA). A specific IgG antibody test using the ELISA is helpful both in suggesting a diagnosis and in ruling out infections. The Centers for Disease Control and Prevention (CDC) currently uses an immunoblotting (IB) test that is highly sensitive and specific for *P. westermani* antibodies. It is based on the demonstration of an 8 kDa antigen–antibody band that is obtained from serum of patients with parasitologically confirmed *P. westermani* infection; the specificity is $\geq$99% [33]. Early diagnosis of the disease is a key consideration for early institution of appropriate treatment to achieve a favorable prognosis. Praziquantel is the drug of choice for both pulmonary and extra-pulmonary paragonimiasis.

There were some limitations to our study that should be mentioned. Firstly, our study was performed retrospectively. Secondly, a small number of patients were included because of the rarity of paragonimiasis. A further limitation is that our study did not differentiate the imaging findings of paragonimiasis to other malignancy. In the future, these limitations will be needed to better understand the features of paragonimiasis.

5. Conclusions

The diagnosis of *P. westermani* infection is difficult because of its complex life cycle and several life stages during infestation of human that results in non-specific clinical presentations, imaging findings and laboratory tests. Recognition and understanding the spectrum of imaging features provide a useful clue for the diagnosis. Integrated with clinical history and laboratory tests, *P. westermani* should be considered in patients with imaging findings of nodules, GGO, worm cyst, migration track, pleural effusion, pleural thickening on chest CT scan; patchy low or mixed density lesions on brain CT scan; ring enhancing lesion on brain MRI scan; conglomerated small cystic or serpentine lesions and migration track in liver and spleen on abdominal CT scan. The characteristic imaging features of paragonimiasis are worm cyst and migration track. However, definitive diagnosis is established by positive findings on a serological test, or detection of eggs or worms in sputum or BAL fluid or stool or in a pathologic specimen. Early diagnosis of the disease is a key consideration for early institution of appropriate treatment to achieve a favorable prognosis.

Acknowledgments

This study was supported by National Key Clinical Specialties Construction Program of China (No. 2013-544).

References

[1] Procop WW. North American paragonimiasis (caused by *Paragonimus kellicotti*) in the context of global paragonimiasis. Clin Microbiol Rev 2009;22:415–46.

[2] Fischer PU, Weil GJ. North American paragonimiasis: epidemiology and diagnostic strategies. Expert Rev Anti Infect Ther 2015;13:779–86.
[3] Keiser J, Utzinger J. Emerging foodborne trematodiasis. Emerg Infect Dis 2005;11:1507–14.
[4] Narain K, Agatsuma T, Blair D. Paragonimus. In: Liu D, editor. Molecular detection of foodborne pathogens. Boca Raton, Florida, USA: CRC Press Taylor & Francis Group; 2010. p. 827–37.
[5] Kim MK, Cho BM, Yoon DY, Nam ES. Imaging features of intradural spinal paragonimiasis: a case report. Br J Radiol 2011;84:e72–4.
[6] Li XM, Yu JQ, He D, Peng LQ, Chu ZG, Chen DD, et al. CT evaluation of hepatic paragonimiasis with simultaneous duodenal or splenic involvement. Clin Imaging 2012;36:394–7.
[7] Tantipalakorn C, Khunamornpong S, Tongsong T. A case of ovarian paragonimiasis mimicking ovarian carcinoma. Gynecol Obstet Investig 2014;77:261–5.
[8] Nakamura-Uchiyama F, Mukae H, Nawa Y. Paragonimiasis: a Japanese perspective. Clin Chest Med 2002;23:409–20.
[9] Nagayasu E, Yoshida A, Hombu A, Horii Y, Maruyama H. Paragonimiasis in Japan: a twelve-year retrospective case review (2001–2012). Intern Med 2015;54:179–86.
[10] Walker MD, Zunt JR. Neuroparasitic infections: cestodes, trematodes, and protozoans. Semin Neurol 2005;25:262–77.
[11] Sahni A, Patel A. IMAGES IN CLINICAL MEDICINE. Hemoptysis associated with *Paragonimus westermani*. N Engl J Med 2015;373:e7.
[12] Xia Y, Ju Y, Chen J, You C. Cerebral paragonimiasis: a retrospective analysis of 27 cases. J Neurosurg Pediatr 2015;15:101–6.
[13] Singh TS, Sugiyama H, Rangsiruji A. Paragonimus & paragonimiasis in India. Indian J Med Res 2012;136:192–204.
[14] Nokolo C. Outbreak of paragonimiasis in Eastern Nigeria. Lancet 1972; 1:32–3.
[15] Im JG, Whang HY, Kim WS, Han MC, Shim YS, Cho SY. Pleuropulmonary paragonimiasis: radiologic findings in 71 patients. AJR 1992; 159:39–43.
[16] Johnson RJ, Johnson JR. Paragonimiasis in Indochinese refugees. Am Rev Respir Dis 1983;128:534–8.
[17] Chai JY. Paragonimiasis. Handb Clin Neurol 2013;114:283–96.
[18] Nawa Y. Re-emergence of paragonimiasis. Intern Med 2000;39:353–4.
[19] Obara A, Nakamura-Uchiyama F, Hiromatsu K, Nawa Y. Paragonimiasis cases recently found among immigrants in Japan. Intern Med 2004;43: 388–92.
[20] Nakamura-Uchiyama F, Onah DN, Nawa Y. Clinical features of paragonimiasis cases recently found in Japan: parasite-specific immunoglobulin M and G antibody classes. Clin Infect Dis 2001; 32:e151–3.
[21] Chen J, Chen Z, Lin J, Zhu G, Meng H, Cui G, et al. Cerebral paragonimiasis: a retrospective analysis of 89 cases. Clin Neurol Neurosurg 2013;115:546–51.
[22] Wang H, Shao B. Imaging manifestations and diagnosis of a case of adult cerebral paragonimiasis with the initial symptom of hemorrhagic stroke. Int J Clin Exp Med 2015;8:9368–73.
[23] Kim EA, Juhng SK, Kim HW, Kim GD, Lee YW, Cho HJ, et al. Imaging findings of hepatic paragonimiasis: a case report. J Korean Med Sci 2004; 19:759–62.
[24] Li XM, Yu JQ, Yang ZG, Chu ZG, Peng LQ, Kushwaha S. Correlations between MDCT features and clinicopathological findings of hepatic paragonimiasis. Eur J Radiol 2012;81:e421–5.
[25] Shim SS, Kim Y, Lee JK, Lee JH, Song DE. Pleuropulmonary and abdominal paragonimiasis: CT and ultrasound findings. Br J Radiol 2012; 85:403–10.
[26] Sasaki M, Kamiyama T, Yano T, Nakamura-Uchiyama F, Nawa Y. Active hepatic capsulitis caused by *Paragonimus westermani* infection. Intern Med 2002;41:661–3.
[27] Singcharoen T, Rawd-Aree P, Baddeley H. Computed tomography findings in disseminated paragonimiasis. Br J Radiol 1988;61:83–6.
[28] Kim KU, Lee K, Park HK, Jeong YJ, Yu HS, Lee MK. A pulmonary paragonimiasis case mimicking metastatic pulmonary tumor. Korean J Parasitol 2011;49:69–72.
[29] Mukae H, Taniguchi H, Matsumoto N, Iiboshi H, Ashitani J, Matsukura S, et al. Clinicoradiologic features of pleuropulmonary *Paragonimus westermani* on Kyusyu Island, Japan. Chest 2001;120: 514–20.
[30] Seon HJ, Kim YI, Lee JH, Kim SH, Kim YH. Differential chest computed tomography findings of pulmonary parasite infestation between the paragonimiasis and nonparagonimiatic parasite infestation. J Comput Assist Tomogr 2015;39:956–61.
[31] Singh TS, Khamo V, Sugiyama H. Cerebral paragonimiasis mimicking tuberculoma: first case report in India. Trop Parasitol 2011;1:39–41.
[32] Kuhlman JE, Fishman EK, Siegelman SS. Invasive pulmonary aspergillosis in acute leukemia: characteristic findings on CT, the CT halo sign, and the role of CT in early diagnosis. Radiology 1985;157:611–4.
[33] Boland JM, Vaszar LT, Jones JL, Mathison BA, Rovzar MA, Colby TV, et al. Pleuropulmonary infection by *Paragonimus westermani* in the United States: a rare cause of Eosinophilic pneumonia after ingestion of live crabs. Am J Surg Pathol 2011;35:707–13.